Polarization-dependent photovoltaic effect in ferroelectric-semiconductor system

Rahmatollah Eskandari,[1,a)] Xiaodong Zhang,[2] and Leszek M. Malkinski[1]
[1]*Department of Physics and Advanced Materials Research Institute, University of New Orleans, New Orleans, Louisiana 70148, USA*
[2]*Department of Chemistry, Tulane University, New Orleans, Louisiana 70118, USA*

(Received 3 December 2016; accepted 3 March 2017; published online 21 March 2017)

Radio-frequency (RF) magnetron sputtering method was used to fabricate ferroelectric films of hafnium oxide doped with 6 mol. % silicon. The effect of polarization of the Si doped HfO_2 layer on photovoltaic properties of this ferroelectric-semiconductor system was investigated. Piezoresponse force microscopy method provided clear evidence for ferroelectric properties of HfO_2 films with 10 nm thickness. Kelvin probe force microscopy showed that change in the surface potential of the negatively poled sample due to illumination is opposite to the response from unpoled and positively poled samples. Transport measurements also revealed a significant difference between photoresponses of the ferroelectric films that were polarized in opposite directions. *Published by AIP Publishing*. [http://dx.doi.org/10.1063/1.4978749]

Photovoltaic phenomenon involves three main processes: light absorption, generation of the electron-hole pairs and separation of the free charges. A suitable semiconductor material with an energy gap in the range of visible light can accomplish the first two steps; however, for the separation of the carriers, more than just a semiconductor medium is required. Conventional solar cells utilize the built-in electric field at the interface of two doped semiconductors (p-n junction) to efficiently separate electrons and holes. This electric field is limited by the energy band gap and alignment of the energy levels of the two joining semiconductors.[1] Additionally, in the junction-based structure, materials' choice is limited due to doping and lattice mismatch issues.[2] To overcome these limits, a new and less explored approach involving ferroelectric materials has been recently gaining attention. Polarization field in ferroelectrics, which can be much larger than built-in electric fields in the depletion layer of a semiconductor p-n junction, can efficiently separate electron-hole pairs.[2–4] Research on photoconductivity in ferroelectrics started four decades ago on famous ferroelectrics such as $BaTiO_3$,[5] $LiNbO_3$[5–7] and $Pb(Zr,Ti)O_3$;[8] however, due to their large band gaps (between 3 and 4 eV), the efficiencies were limited by small current densities negating the effect of their large open circuit photovoltages. In the recent years, the discovery of photoconductivity in smaller band gap ferroelectrics such as $BiFeO_3$ (Refs. 9–11) ($E_g \sim 2.67$ eV (Ref. 11)) has given new promises for the higher efficiency in ferroelectric solar cells.

Various efforts have been taken to realize charge separation in solar cells based on ferroelectric materials. In the simplest designs, besides the separation of charges, a ferroelectric layer sandwiched between two electrodes[12–14] acts also as the source of electron-hole pairs. It has been shown that above band gap voltages can be observed only when the current flows perpendicular to the domain walls of the ferroelectric; otherwise, the response to the light is limited to the photoconductivity of the ferroelectric material.[14] In these cells, however, the efficiency is still more than an order of magnitude smaller than those of commercial cells, mainly because of low quantum efficiency, large band gap and high resistivity of the ferroelectrics.[4,15,16]

An alternative approach is to incorporate low band gap semiconductors inside ferroelectric matrix to improve quantum efficiency. The drawback of this design are the trapping states that are introduced into the band gap.[17,18] In another design, Liu *et al.*[2] utilized polarization field from ferroelectric layer to create positive and negative bound charge sites on the surface of the adjacent semiconductor to separate electron-hole pairs and drive them along the surface of the semiconductor. In their design of solar cell, the free charges generated inside the semiconductor were collected on electrode without entering the ferroelectric medium. Therefore, their concept cannot be easily implemented to improve conventional p-n junction solar cells. In our case, the charges are photogenerated in the semiconductor traverse ferroelectric layer. This makes it possible to integrate the ferroelectric layer with p-n junction based solar cells.

Organic photovoltaics have also benefitted from ferroelectric polymers such as P(VDF-TrFE).[19,20] The polarization field from ferroelectric layer seems to obviate the need for an external bias and enhances the charge separation, although the ferroelectric polymer needs to be very thin (less than 10 nm) in order to facilitate tunneling of the charge carriers.[20] In our approach, the polarization field from a very thin inorganic ferroelectric film of doped hafnium dioxide (~10 nm) is used to separate free charge careers produced inside the semiconductor, and low thickness of the film allows the careers to tunnel across the ferroelectric film. This method can be potentially exploited to enhance the efficiency of p-n junction solar cells by enhancing the electric field in the vicinity of the depletion zone.

Ferroelectricity has recently been reported in hafnium dioxide (HfO_2) thin films doped with Si[21] and other elements.[22,23] Hafnia crystallizes in four phases: monoclinic, cubic, tetragonal

a)Author to whom correspondence should be addressed. Electronic mail: reskanda@uno.edu

and orthorhombic phases with the monoclinic phase being the most stable phase. Other phases need extreme conditions such as high temperature or pressure to be stabilized.[24] Before the discovery of ferroelectricity in HfO_2, all phases were known to be centrosymmetric and non-polar, which excluded ferroelectricity in hafnia.[25] Therefore, new polar orthorhombic phases were proposed[21] based on the comparison of experimental results with similar compounds such as ZrO_2, and later, theoretical calculations[26] confirmed the possibility of those phases. It has been shown that capping layer and doping such as addition of 5–10 mol. % of Si can stabilize other phases including the polar phase of hafnia at ambient conditions.[27,28]

A variety of methods such as ion-assisted deposition (IAD),[29] metal organic atomic layer deposition (MOALD)[21] and atomic layer deposition (ALD)[30] were suggested and utilized to prepare ferroelectric HfO_2 thin films.

In this article, we discuss the synthesis and physical properties of ferroelectric thin films of HfO_2 on Si. We describe the technology of 10 nm thick ferroelectric films of Si-doped hafnia, which is based exclusively on magnetron sputtering. We report on discovery of polarization-dependent photovoltaic effect in this ferroelectric/semiconductor system. The photo-response measurements using Kelvin probe force microscopy (KPFM) and I–V curves indicate possibility of implementing poled ferroelectric HfO_2 films into solar cell structures to enhance their performance.

Hafnium dioxide thin films doped with silicon and capped with titanium nitride (TiN) layer were fabricated by RF magnetron sputtering. Two-inch diameter metallic hafnium target (99.9% pure, K.J. Lesker) with a small piece of silicon wafer that was mounted on its surface was used as the sputtering target. Silicon (001) substrates were cleaned according to the solvent clean procedure, followed by 2 min dip in hydrofluoric acid (HF, 4 vol. %) in order to remove native oxide. Vacuum system Orion-8 (AJA International) was pumped down to pressures below 5.0×10^{-8} Torr, and substrates were heated up to 300 °C for 5 min prior to deposition in order to acquire a uniform temperature on the entire wafer. Silicon doped HfO_2 films were RF sputtered at the rate of 63 Å/min using gun power of 150 W. During the deposition, the gas ratio of $Ar:O_2 = 90:10$ was maintained at the pressure of 3 mTorr. TiN layer with 20 nm thickness was also sputtered on top of doped HfO_2 film using the RF power of 150 W with a gas ratio of $Ar:N_2 = 95:5$, at the deposition pressure of 2 mTorr and deposition rate of 20 Å/min. Substrates were kept at 300 °C and rotated during all depositions to ensure the uniformity of the films. The thickness of all films was individually calibrated and confirmed using reflectometry (Filmetrics, F20) and scanning probe microscopy (Asylum Research, MFP-3D) techniques. Ultimately, films were annealed at 800 °C for 20 s using rapid thermal annealing (RTA) system (ULVAC-RIKO, model MILA-5000) under nitrogen ambient to introduce desired crystallinity with ferroelectric phase.[28]

In order to determine the Si/Hf mole ratio, a thicker film of doped hafnia was deposited at the same conditions on a sapphire substrate, and X-ray photoelectron spectroscopy (XPS) measurement was carried out on a VG Scientific MKII system with an Al Kα anode as the excitation source ($h\nu = 1486.6$ eV). Obtained peaks via XPS were fitted with a custom VBA program in Microsoft Excel using the Voigt profiles together with a Shirley background function. The results showed the Si/Hf ratio of about 6 mol. % in the samples.

Tracking the crystal structure of the films in our samples with XRD method confirmed the phase transition from monoclinic to orthorhombic in the presence of the silicon dopant and capping layer. Samples right after deposition at 300 °C did not show any ferroelectricity, and ferroelectricity in the films occurred only after annealing of the samples at 800 °C, thus confirming the crystallization in the form of the polar orthorhombic phase. It has been found that the formation of tetragonal and orthorhombic phases was strongly influenced by the dopant and capping layers. The XRD graphs are presented in supplementary material.

Polarization switching of the domains of the film by the means of dual AC resonance-tracking piezoresponse force microscopy (DART-PFM) technique was used to examine local ferroelectric properties of the film. For this purpose, TiN layer was selectively etched with a diluted standard clean (SC-1) solution (NH_4OH (50 vol. %):H_2O_2 (30%):H_2O ~ 1:1:10) at 40 °C to expose doped hafnia film. The imaging process was carried out after the sample was subjected to 10 000 cycles of a bipolar wave with the magnitude of 5 V and the frequency of 100 Hz in order to complete the ferroelectricity wake up and improve the polarizability. The PFM measurements were carried out using a conductive silicon cantilever with titanium/platinum coating (OMCL-AC240TM-R3, the resonant frequency of 70 kHz and spring constant~2 N/m). PFM lithography technique was used to write two nested squares with the sizes of 10 μm and 5 μm (as shown in Fig. 1(a)) by applying the voltage to the conductive cantilever. The larger square was written by −5 V and inner square with +5 V applied to the tip, while the sample was grounded. Fig. 1(a) shows the phase image of the pattern obtained by PFM after lithography and dashed squares correspond to the locations of the oppositely polarized regions. Fig. 1(b) is the corresponding amplitude image from the same area, as shown in Fig. 1(a). Both of these images confirm the ferroelectric properties and domain switching in the film by applying electric fields.

Macroscopic ferroelectric properties were accessed via ferroelectric hysteresis measurements. A 30 nm thick gold layer was deposited via electron beam evaporation on top of TiN layer, and square electrodes with the dimensions of 50 μm × 50 μm were created using photolithography methods. Gold layer was etched away with KI (saturated in H_2O) + HIO_3 (1.0 wt. %) solution at ambient temperature, and then TiN layer was selectively etched with diluted SC-1 solution.

Hysteretic behavior of the film under applied electric field is shown in Figs. 1(c) and 1(d). Figure 1(c) represents the phase change versus applied voltage. Phase change close to 180° was observed when the voltage of the tip changed from −5 V to +5 V. Figure 1(d) shows the displacement of the film surface with applied voltage. As expected, the displacement diagram has a butterfly-shaped hysteresis. The piezoresponse mapping and hysteresis measurements together satisfy the ferroelectricity criteria and rule out the

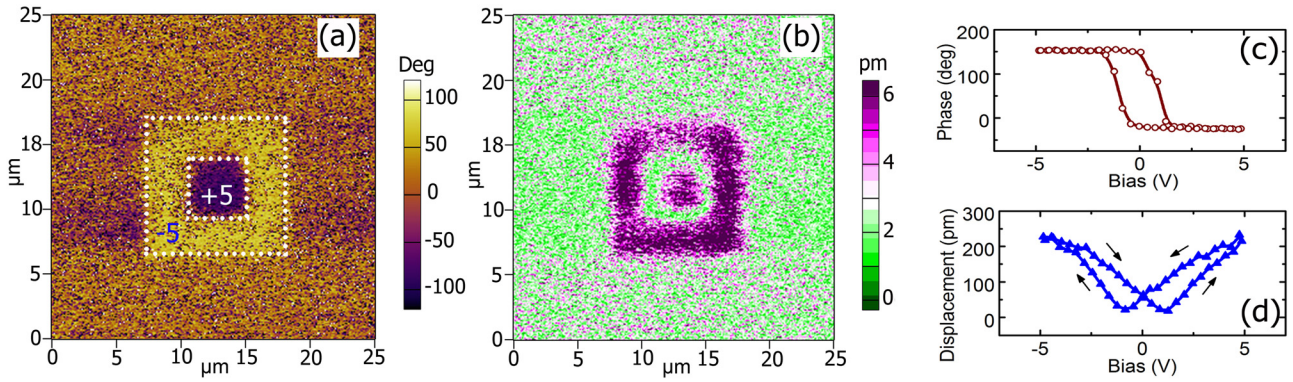

FIG. 1. Piezoresponse force microscopy (PFM) of the TiN-etched surface of the Si:HfO_2 film: (a) phase image of the poled surface with corresponding poling pattern, larger dashed square was poled with −5 V bias and smaller square was poled with +5 V; (b) corresponding amplitude image for the same area; (c) and (d) represent phase and displacement hysteresis graphs obtained from the top of the gold square electrodes.

possibility of the hysteresis effect due to the charge trapping phenomenon.[31]

In order to investigate the possibility of ferroelectric HfO_2 films to be incorporated into the structure of photovoltaic cells, first, we need to polarize the films, so we can employ that polarization field for the separation of the carriers. To this end, three pieces from the same ferroelectric sample (10 nm thick, 6 mol. % Si) were cut and two of them were exposed to a high electric field at room temperature. These two pieces were poled in opposite directions using the poling setup that is schematically depicted in Fig. 2(c). The samples were placed between two 0.1 mm thick glass slides, separating them from electrodes. The voltage of 5 kV was applied between electrodes with the separation equal to 1 mm. The poling direction was defined as positive for the sample with the substrate (Si) at the negative electrode (anode) side and HfO_2 film close to the positive electrode (cathode) leading to an upward (from the substrate to the film) polarization direction. For the negative poling, the sample was flipped over, so the polarization direction was downward (from film towards the substrate).

All three samples were studied by measuring their surface potential in the dark (OFF mode) and under the light (ON mode) using Kelvin probe force microscopy (KPFM) method. The voltage of 2 V was applied to a platinum coated conductive cantilever that was oscillating at the resonant frequency (∼60 kHz), and potential of the surface was recorded in nap mode (tip was lifted about 20 nm from the surface). In order to measure the response from the same location of the sample, scanning was performed along a 2 μm line (vertical direction in Fig. 2(a)) and the horizontal scan was disabled.

Figure 2(a) shows the surface potential for the positively poled sample. During the scan, the light (remotely provided by optical fiber from 150 W tungsten halogen lamp) was turned on and off in an equal time-frames, so the results could be comparable for negatively poled and unpoled samples. In Fig. 2(b), the cross-section of the image that is averaged over the total length of the scan along with the results of the unpoled and negatively poled samples is presented. As evidenced by cross section (Fig. 2(b)), polarization introduced an obvious change in the way that polarized and unpolarized samples responded to the light. Negatively poled sample responds to the light in an opposite way compared to the positively poled and unpoled samples. In positively poled and unpoled samples, surface potential decreases when the light turns on, while negatively poled sample shows an increase in surface potential.

It is worth to mention that KPFM is a quasi-quantitative method and the measured values representing the difference between the potential of the tip and the surface are not absolute. The change in surface potential under illumination

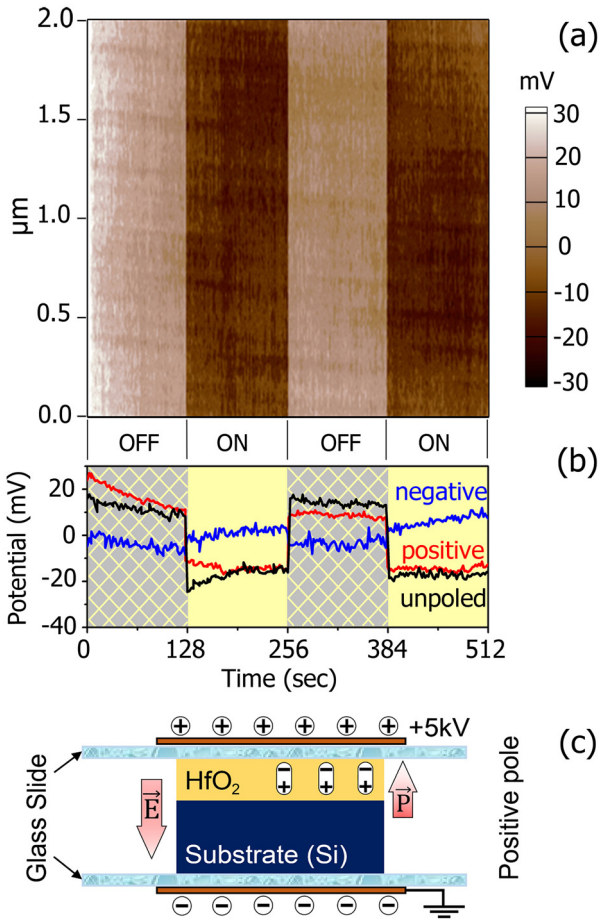

FIG. 2. KPFM of the TiN-etched surface of the Si:HfO_2 thin film. (a) Surface potential of the positively poled film at OFF-ON-OFF-ON conditions. (b) Corresponding surface profile which is averaged over the entire length of the region (red line). Results from negatively poled sample (blue line) and unpoled sample (black line) are also included for comparison. (c) Schematic representation of the setup for positive poling.

shows the photoconductivity response of the sample; however since there is no actual current passing across the film, due to the large band gap of the HfO_2 film, charge carriers are expected to face a high barrier in an actual cell. Therefore, complementary measurements were carried out to study the tunneling and carrier transport across the lamellar structure. A complete cell was fabricated by formation of a semi-transparent electrode by evaporating 5 nm of gold on top of the HfO_2 film, and current-voltage (I–V) curves were recorded using picoammeter (Keithley 2614B Sourcemeter unit), while cells were exposed to simulated AM1.5 spectrum from the light source.

The I–V diagrams of the three samples under AM1.5 illumination are presented in Fig. 3. The polarized samples showed opposite changes in the I–V characteristics, as compared to the unpoled sample. Open-circuit voltages (V_{oc}) have been improved for negatively poled sample, while positive poling seemed to diminish the open-circuit voltage and short-circuit current (J_{sc}).

In order to identify the source of photo-generated carriers, supplementary photoconductivity measurements were carried out on the surface of doped HfO_2 (~200 nm thick) using the four-point probe system. The resistivity of HfO_2 had no change under illumination. This concludes that the lower band gap media such as silicon is the source of generated electron-holes, and the polarization field from ferroelectric film separates them and drives in opposite directions, thus explaining the occurrence of the photovoltaic effect in the Si/HfO_2 system.

In summary, we developed the technology of fabrication of ferroelectric hafnia films doped with silicon by magnetron sputtering. Ferroelectric properties were verified by domain switching using PFM methods. We have demonstrated that the performance of ferroelectric-semiconductor solar cells can be enhanced by polarizing thin ferroelectric films in a proper direction. KPFM and I–V measurements showed that photogeneration takes place inside the Si layer adhering to the ferroelectric film of HfO_2. On the other hand, highly resistive HfO_2 layer with larger band gap did not show any trace of photoconductivity. For these reasons, the occurrence of the photovoltaic effect in the Si/HfO_2 system can be ascribed to the existing ferroelectric layer. The role of the electric fields that separate photogenerated carriers and direct them towards solar cell electrodes was revealed by using different polarization directions of the ferroelectric layer. Although the design of the cells presented in this work was not optimized, it can be speculated that the mechanism of generating or enhancing the photovoltaic effect by the means of electric field from the ferroelectrics can lead to a new generation of solar cells. It is expected that the efficiency of such cells can be greatly enhanced by fabricating multilayered structures. It is important to mention that our results indicate a great potential of ferroelectric layers to be implemented in conventional cells to enhance voltage in p-n junction based solar cells.

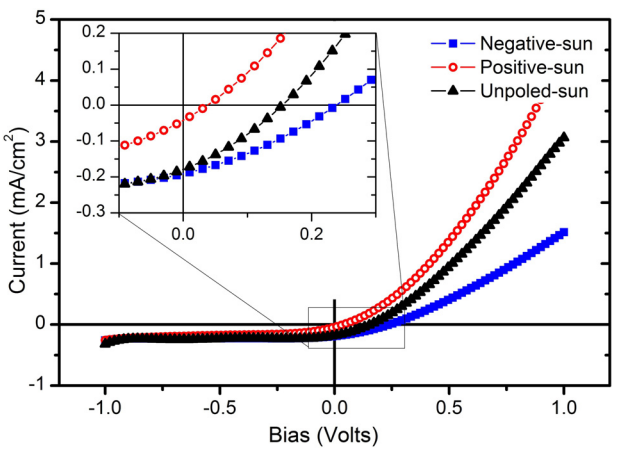

FIG. 3. Current density-voltage characteristic of the $Si/HfO_2/Au$ cell. The inset is the magnified depiction of the identified region close to the zero bias voltage.

See supplementary material for XRD characterization results of HfO_2 films synthesized at different conditions.

The authors would like to acknowledge the support from NSF EPSCoR LA-SiGMA Cooperative Agreement No. EPS-1003897 along with the additional support from the Louisiana Board of Regents through Contract NSF (2010-15)-RII-UNO and SCORE 2012 grant from UNO.

[1]P. Würfel, *Physics of Solar Cells: From Basic Principles to Advanced Concepts*, 2nd ed. (Wiley-VCH, 2009).
[2]F. Liu, W. Wang, L. Wang, and G. Yang, Appl. Phys. Lett. **104**, 103907 (2014).
[3]M. Alexe and D. Hesse, Nat. Commun. **2**, 256 (2011).
[4]S. Y. Yang, J. Seidel, S. J. Byrnes, P. Shafer, C.-H. Yang, M. D. Rossell, P. Yu, Y.-H. Chu, J. F. Scott, J. W. Ager, L. W. Martin, and R. Ramesh, Nat. Nanotechnol. **5**, 143 (2010).
[5]V. M. Fridkin and B. N. Popov, Sov. Phys. – Usp. **21**, 981 (1978).
[6]A. M. Glass, D. von der Linde, and T. J. Negran, Appl. Phys. Lett. **25**, 233 (1974).
[7]A. M. Glass, D. von der Linde, D. H. Auston, and T. J. Negran, J. Electron. Mater. **4**, 915 (1975).
[8]P. S. Brody and F. Crowne, J. Electron. Mater. **4**, 955 (1975).
[9]S. R. Basu, L. W. Martin, Y. H. Chu, M. Gajek, R. Ramesh, R. C. Rai, X. Xu, and J. L. Musfeldt, Appl. Phys. Lett. **92**, 091905 (2008).
[10]T. Choi, S. Lee, Y. J. Choi, V. Kiryukhin, and S. W. Cheong, Science **324**, 63 (2009).
[11]S. Y. Yang, L. W. Martin, S. J. Byrnes, T. E. Conry, S. R. Basu, D. Paran, L. Reichertz, J. Ihlefeld, C. Adamo, A. Melville, Y. H. Chu, C. H. Yang, J. L. Musfeldt, D. G. Schlom, J. W. Ager, and R. Ramesh, Appl. Phys. Lett. **95**, 062909 (2009).
[12]D. Cao, C. Wang, F. Zheng, W. Dong, L. Fang, and M. Shen, Nano Lett. **12**, 2803 (2012).
[13]M. Qin, K. Yao, and Y. C. Liang, Appl. Phys. Lett. **93**, 122904 (2008).
[14]J. Seidel, D. Fu, S. Y. Yang, E. Alarcón-Lladó, J. Wu, R. Ramesh, and J. W. Ager, Phys. Rev. Lett. **107**, 126805 (2011).
[15]L. Pintilie, I. Vrejoiu, G. Le Rhun, and M. Alexe, J. Appl. Phys. **101**, 064109 (2007).
[16]K. Yao, B. K. Gan, M. Chen, and S. Shannigrahi, Appl. Phys. Lett. **87**, 212906 (2005).
[17]X. Yang, X. Su, M. Shen, F. Zheng, Y. Xin, L. Zhang, M. Hua, Y. Chen, and V. G. Harris, Adv. Mater. **24**, 1202 (2012).
[18]D. Shvydka and V. G. Karpov, Appl. Phys. Lett. **92**, 053507 (2008).
[19]K. Asadi, P. de Bruyn, P. W. M. Blom, and D. M. de Leeuw, Appl. Phys. Lett. **98**, 183301 (2011).
[20]Y. Yuan, T. J. Reece, P. Sharma, S. Poddar, S. Ducharme, A. Gruverman, Y. Yang, and J. Huang, Nat. Mater. **10**, 296 (2011).
[21]T. S. Böscke, J. Müller, D. Bräuhaus, U. Schröder, and U. Böttger, Appl. Phys. Lett. **99**, 102903 (2011).
[22]J. Müller, T. S. Böscke, D. Bräuhaus, U. Schröder, U. Böttger, J. Sundqvist, P. Kücher, T. Mikolajick, and L. Frey, Appl. Phys. Lett. **99**, 112901 (2011).

[23]J. Müller, U. Schröder, T. S. Böscke, I. Müller, U. Böttger, L. Wilde, J. Sundqvist, M. Lemberger, P. Kücher, T. Mikolajick, and L. Frey, J. Appl. Phys. **110**, 114113 (2011).
[24]J. Wang, H. P. Li, and R. Stevens, J. Mater. Sci. **27**, 5397 (1992).
[25]M. E. Lines and A. M. Glass, *Principles and Applications of Ferroelectrics and Related Materials* (Oxford University Press, 2001).
[26]T. D. Huan, V. Sharma, G. A. Rossetti, and R. Ramprasad, Phys. Rev. B **90**, 064111 (2014).
[27]K. Tomida, K. Kita, and A. Toriumi, Appl. Phys. Lett. **89**, 142902 (2006).
[28]E. Yurchuk, J. Müller, S. Knebel, J. Sundqvist, A. P. Graham, T. Melde, U. Schröder, and T. Mikolajick, Thin Solid Films **533**, 88 (2013).
[29]J. P. Lehan, Y. Mao, B. G. Bovard, and H. A. Macleod, Thin Solid Films **203**, 227 (1991).
[30]D. H. Triyoso, P. J. Tobin, B. E. White, R. Gregory, and X. D. Wang, Appl. Phys. Lett. **89**, 132903 (2006).
[31]L. Pintilie and M. Alexe, Appl. Phys. Lett. **87**, 112903 (2005).